J Solid State Electrochem (2006) 10: 18–23
DOI 10.1007/s10008-005-0647-9

ORIGINAL PAPER

Myoung-Sup Kim · Joon-Hyung Lee
Jeong-Joo Kim · Hee Young Lee
Sang-Hee Cho

Microstructure evolution and dielectric properties of $Ba_{5-x}Na_{2x}Nb_{10}O_{30}$ ceramics with different Ba–Na Ratios

Received: 28 September 2004 / Revised: 4 October 2004 / Accepted: 6 December 2004 / Published online: 4 March 2005

Abstract The tetragonal tungsten bronzes of $Ba5-x$-$Na_{2x}Nb_{10}O_{30}$ (BNN, $0.5 \leq x \leq 1.3$) ceramics were synthesized using the solid state reaction method. The sintering behavior and dielectric characteristics of the BNN ceramics, as a function of the Ba-Na ratio, were examined. Densification of the samples with excess compositions of Ba and Na was higher than that of the stoichiometric BNN sample. The maximum dielectric constant and the Curie temperature showed highest values at the stoichiometric composition and decreased as the composition shifted away from the stoichiometry. in order to obtain a quantitative evaluation of the diffuse phase transition (DPT) behavior of the BNN ceramics, γ and C/κ_{max} were calculated. The weakest DPT behavior was observed in the stoichiometric composition. An increase in the DPT is in correlation with the increase in the number of ways of cation distribution by the disordered occupation of Ba and Na and the vacancies in the A1 and A2 sites of the tungsten bronze structure.

Keywords Tungsten bronze structure · BNN · Ferroelectrics · DPT · Order–disorder

Introduction

The tungsten bronze structure consists of [1, 2] a skeleton framework of the MO_6 octahedral, sharing corners to form three different types of tunnels parallel to the *c*-axis in the unit cell formula of $[(A1)_2(A2)_4C_4][(B1)_2(B2)_8]O_{30}$. Various tungsten bronze families exist. One of the basic differences between the tungsten bronze families is the attributed to A-site and/or C-site cation occupancy, which is determined by the ionic valence, coordination number, and radius. Among the various tungsten bronze families, the empty bronzes have the partially filled A-sites. This type is characterized by $Sr_{1-x}Ba_xNb_2O_6$(SBN), which has five-sixth occupancy (i.e., one-sixth vacancy) in the A-site and an empty C-site. There are other family members that have all A-site positions occupied, which are known as filled bronzes. These are characterized by $Ba_2NaNb_5O_{15}$ (BNN) and $K_3Li_2Nb_5O_{15}$ (KLN); however, the C-site of BNN is empty, while KLN is completely filled, where K^+ occupies both the A1 and A2 sites, Li^+ occupies the C-site, and Nb^{5+} occupies both the B1 and B2 sites. These various cation occupation formule are believed to affect their physical and chemical properties greatly.

In the case of ferroelectric BNN ceramics, which have high electro-optic, piezoelectric, and nonlinear optical efficiencies,[3–5] the space of the A1 site is smaller than that of the A2 site. Therefore, it has been generally accepted that Ba occupies the A2 site, and Na occupies the A1 site, since the Na ion radius is smaller than that of Ba.[6, 7] In this case, when the Ba–Na ratio varies, the occupancy, distribution, and ordering of Ba, Na and the vacancy at the A1 and A2 sites in the unit cell of tungsten bronze will be changed accordingly. This obviously will affect the dielectric characteristics of the BNN ceramics.

In this study, the sintering behavior, microstructure evolution, dielectric characteristics, Curie temperature and the DPT behavior of the BNN ceramics as a function of the Ba–Na ratio were examined. The diffuseness of the dielectric constant, which is a measure of the degree of DPT, and the number of possible ways of cation distribution (distribution possibilities), which is also related to the degree of DPT, were calculated. The

M.-S. Kim · J.-H. Lee · J.-J. Kim (✉) · S.-H. Cho
Department of Inorganic Materials Engineering Kyungpook, National University,
Daegu, 702-701, Korea
E-mail: jjkim@knu.ac.kr
Tel.: +82-53-9505635
Fax: +82-53-9505645

H. Y. Lee
Department of Materials Science and Engineering, Yeungnam University, Gyeongsan,
712-749, Korea

theoretical calculations of the cation site occupation and the experimental results are compared and discussed.

Experimental procedure

The starting powders of $Ba_{5-x}Na_{2x}Nb_{10}O_{30}$, where x = 0.5–1.3, were prepared using high purity raw materials of $BaCO_3$ (99.95%), Na_2CO_3 (99.5%), and Nb_2O_5 (99.9%) by the general solid state reaction process. The compositions of the starting powders were divided into Ba excess ($x = 0.5$–0.9), Na excess ($x = 1.1$–1.3), and the stoichiometric $Ba_4Na_2Nb_{10}O_{30}$ (BNN, $x = 1.0$). The weighed powders were wet mixed for 24 h in a plastic jar with zirconia balls and ethanol. After drying, the mixtures were calcined at 1,200 °C for 2 h. The calcined powders were wet ball-milled again for crushing. After drying, the powders were formed into pellets by a sequential process of uniaxial pressing followed by cold isostatic pressing (CIP) at 100 MPa for 3 min.

Samples were sintered in the temperature range of 1,200–1,375 °C for 2 h with a heating rate of 5 °C/min. The crystal structure and phase evolution were identified by an X-ray diffractometer (M03XHF, Mac Science, Japan) using Cu-K_α radiation. The density of the sintered samples was determined by the Archimedes method and the microstructure of the polished samples was observed using a scanning electron microscope (SEM; JEOL, JML5400, Tokyo, Japan) after thermal etching. The average grain size of the sample was determined by the linear intercept method[8]. For dielectric measurements, an Ag electrode was screen-printed on the both surfaces of the sintered samples, and fired at 600 °C for 10 min. The dielectric properties were analyzed by an impedance gain phase analyzer (HP4194A, U.S.A.) with a frequency increment in step from 1 kHz to 1 MHz in the temperature range from 100 °C to 700 °C, with temperature increments of 2 °C.

Results and discussion

Figure 1 shows the powder X-ray diffraction patterns of the samples calcined at 1,200 °C for 2 h as a function of the Ba–Na ratio. The typical diffraction patterns of BNN were observed. In the case of $x = 0.5$ and 1.3, however second phases of $BaNb_2O_6$ and $NaNbO_3$, which were anticipated to appear from the phase diagrams of the $NaNbO_3$–$BaNb_2O_6$ system [9, 10] were observed, respectively.

Figure 2 shows the variation of lattice parameters and the axial ratio with the compositions over the range from $x = 0.5$ to 1.3. The lattice parameters a and c, and the axial ratio of °C10· c/a decreased with an increase in the Na content from $x = 0.5$ to 1.1. They then increased slightly with a further increase of x to 1.3. The decrease in the lattice parameters a and c is believed to be caused by the different ionic radii of Ba^{2+} (1.47Å, CN = 9) and Na^+ (1.32Å, CN = 9). Although excess Ba creates Na vacancies in the structure, the influence on the lattice constant seems insignificant.

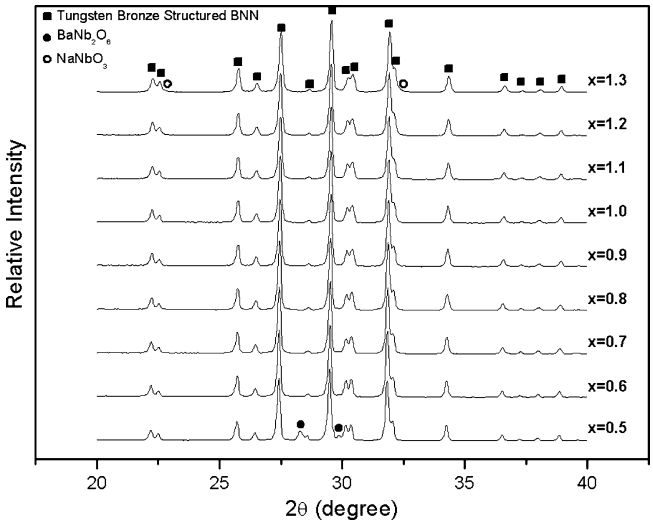

Fig. 1 X-ray diffraction patterns of BNN samples calcined at 1,200 °C for 2 h with different x in $Ba_{5-x}Na_{2x}Nb_{10}O_{30}$

Figure 3 shows the relative density of the samples sintered at 1,300 °C for 2 h as a function of the Ba–Na ratio. Even though the stoichiometric BNN showed low density, around 88%, Ba excess or Na excess compositions resulted in a higher density of 95% and 91%, respectively, in that the stoichiometric BNN, as the content of excess, increased. The higher densification of the Ba excess composition compared with the stoichiometric composition is believed to be caused by the generation of cation vacancies in the structure, which provides easier diffusion paths. When one excess Ba^{2+} ion is added, two Na^+ ions will come out in order to satisfy charge neutrality. In this case, cation vacancies can be produced in the lattice. Since the vacancies accelerate mass transfer, the improved densification is believed to arise from increased diffusivity or lowered activation energy for atomic diffusion. In the case of Na excess samples, since all of the excess Na cannot be squeezed into the crystal of the tungsten bronze structure, as the number of A sites is limited to six, some of the Na ions must remain in the sample, which is thought to produce second phases with low melting temperatures. According to the phase relationship in the Na_2O–Nb_2O_5 system[11], the melting temperature of the phases ranges from 975 °C (Na excess composition) and 1,220 °C (Nb excess composition) to 1,412 °C (Na:Nb = 1:1 composition). The liquid phase from the second phases seems to contribute to the densification of the Na excess samples.

Table 1 shows the variation of occupancy at the A1 and A2 sites of tungsten bronze structured BNN as a function of the Ba–Na ratio. In the stoichiometric BNN, two A1 and four A2 sites are completely filled with Na and Ba ions, respectively. When excess Ba is added, for example, when one excess Ba^{2+} ion substitutes for two Na^+ ions at the A1 site, one Na^+ ion among the two

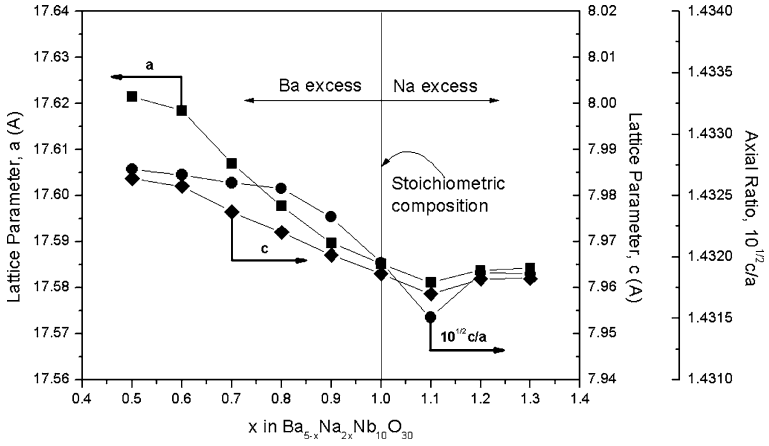

Fig. 2 Variation of lattice parameters and axial ratio of BNN samples calcined at 1,200 °C for 2 h as a function of x in $Ba_{5-x}Na_{2x}Nb_{10}O_{30}$

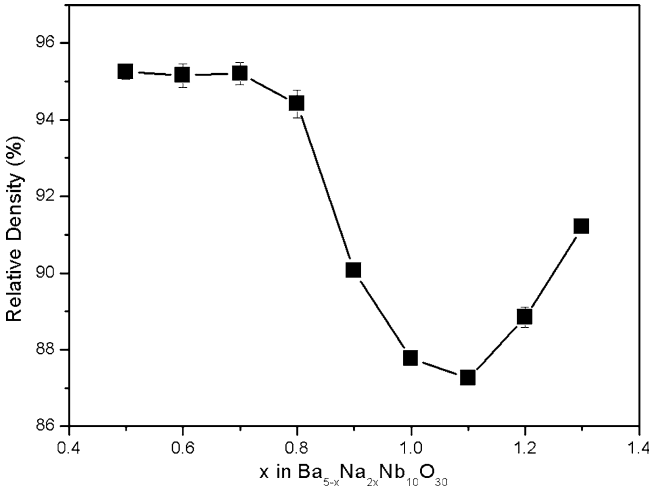

Fig. 3 Relative density of BNN samples sintered at 1,300 °C for 2 h as a function of x in $Ba_{5-x}Na_{2x}Nb_{10}O_{30}$

Table 1 Variation of occupancy at the A1, A2 sites of tungsten bronze structure with different x in $Ba_{5-x}Na_{2x}Nb_{10}o_{30}$

x	A2 site			A1 site			Remain	
	Occupancy		Vac.	Occupancy		Vac.		
	Ba	Na		Ba	Na		Ba	Na
0.6	4	0	0	0.4	1.2	0.4	0	0
0.8	4	0	0	0.2	1.6	0.2	0	0
1	4	0	0	0	2	0	0	0
1.2	3.8	0.2	0	0	2	0	0	0.2

will be expelled, introducing a Na vacancy at the A1 site. In the case of Na excess compositions, when $x = 1.2$, there should remainsome Na^+ ions which cannot enter the crystal structure.

Figure 4 shows the microstructure of the samples sintered at 1,300 °C for 2 h as a function of the Ba–Na ratio. In the case of Ba excess composition, the relative density was over 95% and the average grain size was about 2.6–3.2 μm. In the case of Na excess and stoichiometric compositions, the relative density was around 87–88% and the average grain size was about 2.4–3.2 μm. It was found that the vacancies in the Ba excess composition did not contribute to grain growth very significantly even though they promoted densification. Moreover, the liquid phase which might be formed in the Na excess composition also did not contribute to the grain growth.

Figure 5 shows the temperature dependence of the dielectric constant of BNN as a function of the Ba–Na ratio. DPT behavior was observed in every composition and the phase transition temperature, as well as the maximum dielectric constant were dependent on the Ba–Na ratio.

The phase transition temperature (Curie temperature) and the maximum dielectric constant at the Curie temperature of the samples as a function of the Ba–Na ratio are presented in Fig. 6. The maximum dielectric constant shows the highest value at the stiochiometric BNN ($x = 1.0$) and it decreased as the composition shifted away from the stoichiometry. The Curie temperature shows the highest temperature at the stoichiometric BNN and it, too, decreased as the composition shifted away from the stoichiometry.

The degree of DPT behavior of the BNN samples can be quantified from Fig. 5. Uchino and Nomura [12] attempted quantification of DPT behavior in terms of the Gaussian distribution of the dielectric constant, using the following equation.

$$\frac{1}{\kappa} - \frac{1}{\kappa_{\max}} = \frac{(T - T_C)^{\gamma}}{C}, \quad (1)$$

where κ is the dielectric constant, $\kappa_{\max}$ is the maximum dielectric constant, T is the temperature, T_C is the Curie temperature, γ is the diffuseness coefficient, and C is the Curie-like constant. By taking the logarithm on both sides of the equation, the relationship between $\log(T - T_c)$ and $\log(1/\kappa - 1/\kappa_{\max})$ can be illustrated, and from the gradient of the graph we can read off the γ value. A high correlation of the γ value with the plane transformation diffuseness was found [12, 13]. The value of γ is accepted empirically as representing a first-order

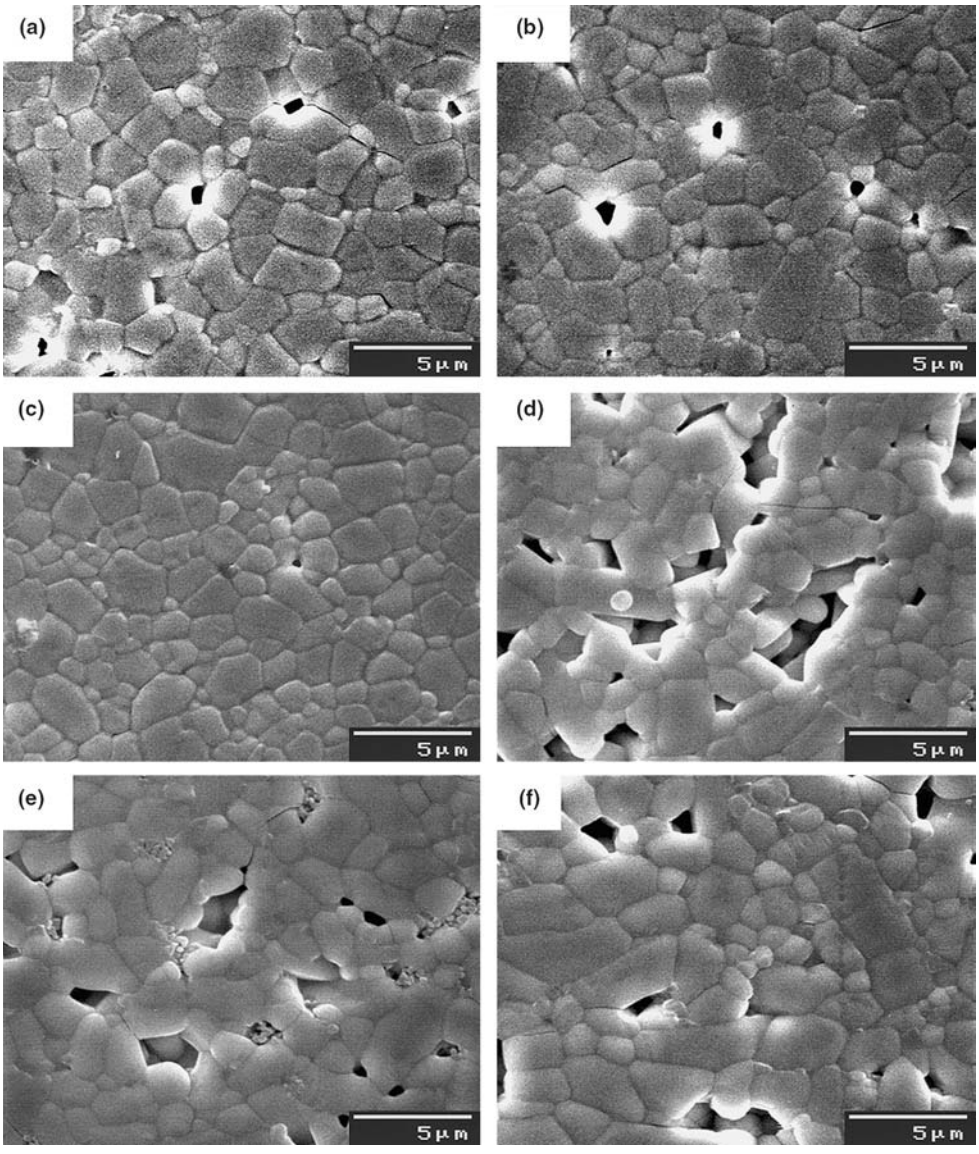

Fig. 4 SEM photographs of BNN samples sintered at 1,300 °C for 2 h with different x in $Ba_{5-x}Na_{2x}Nb_{10}O_{30}$. (**a**) $x = 0.5$, (**b**) $x = 0.7$, (**c**) $x = 0.8$, (**d**) $x = 1.0$, (**e**) $x = 1.2$ and (**f**) $x = 1.3$

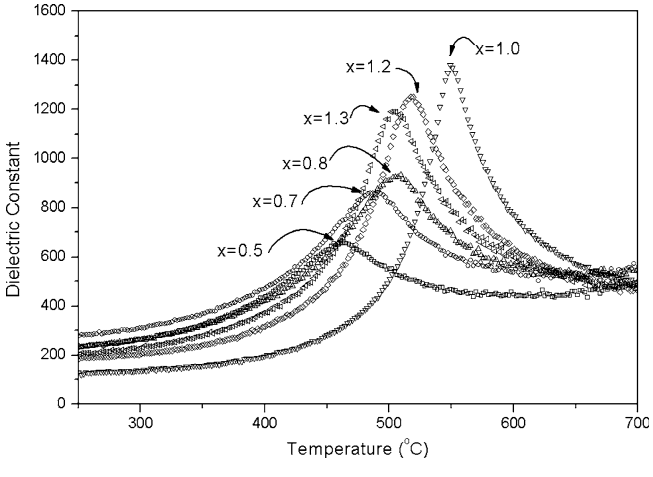

Fig. 5 A comparison of dielectric constant of samples sintered at 1,300 °C for 2 h measured at 100 kHz with different x in $Ba_{5-x}Na_{2x}Nb_{10}O_{30}$

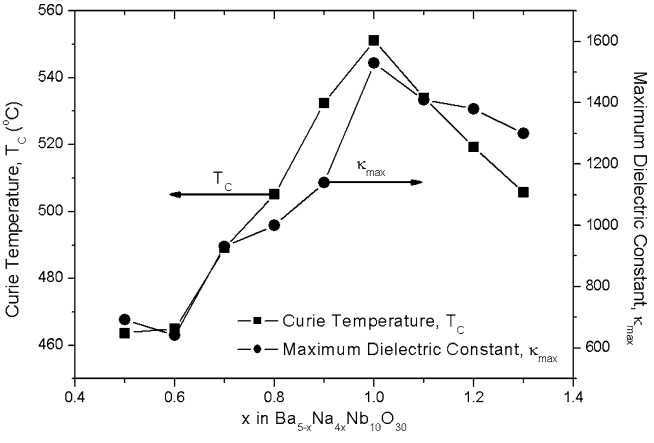

Fig. 6 Variation of the T_C and κ_{max} of samples sintered at 1,300 °C for 2 h as a function of x in $Ba_{5-x}Na_{2x}Nb_{10}O_{30}$

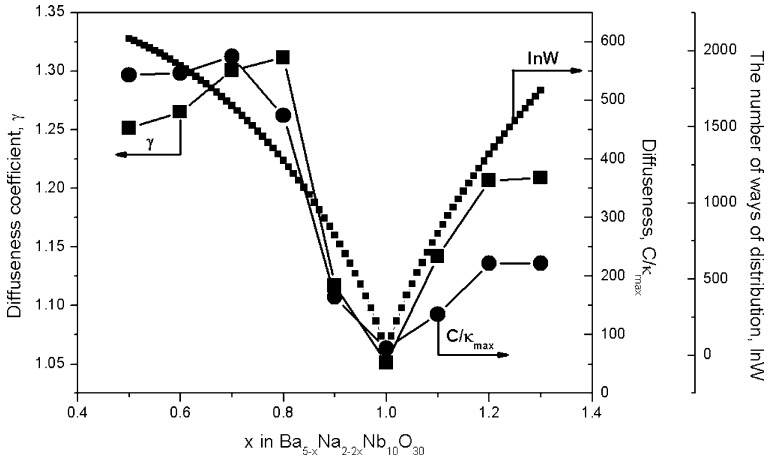

Fig. 7 Variation of the diffuseness coefficient (γ), diffuseness (C/κ_{max}) of samples and the number of ways of distribution of samples sintered at 1,300 °C for 2 h as a function of x in $Ba_{5-x}Na_{2x}Nb_{10}O_{30}$

phase transformation when it is 1 and a second-order phase transformation when it is 2 [12]. Equation 1can be expressed as follows.

$$\frac{\kappa_{max}}{\kappa} = 1 + \frac{\kappa_{max}}{C}(T - T_C)^{\gamma} \quad (2)$$

Let the value of γ obtained from Equation 1 be substituted into Equation 2. Then, the relationship between κ_{max}/κ and $(T-T_C)^{\gamma}$ can be derived. From the gradient of the graph, the reciprocal gradient C/κ_{max} is obtained and this represents the measure of the diffuseness, as the fall-off rate of κ/κ_{max}.

The Variation of γ and C/κ_{max} values with respect to the Ba–Na ratio are summarized in Fig. 7. The lowest value of γ was exhibited by the stoichiometric BNN, but this increased when the Na content went further from the stoichiometry. The value of C/κ_{max} was also marked at its lowest at the stoichiometric BNN. This signifies that the stoichiometric BNN approaches first-order phase transformation and the degree of DPT decreases as well. The degree of DPT can be explained by the degree of disorder of Ba and Na ion in the A1 and A2 sites, because the degree of disorder is directly related with the DPT behavior[14, 15].

In the stoichiometric BNN ceramics, six A sites (four A2 sites and two A1 sites) are fully occupied by four Ba and two Na ions. In the case of Ba excess compositions ($x = 0.9$–0.5), the disordering of the A1 sites will be increased due to the incorporation of Ba ions together with the Na vacancies. In the case of Na excess compositions ($x = 1.1$–1.3), however, surplus cations for the A sites will remain. When some of the excess Na ions are substituted for Ba ions in the A2 sites, the disordering of the A2 sites will be increased. Therefore, we can estimate the degree of disordering in the BNN ceramics from the occupation behavior of the cations, which will be increased as the composition goes away from the stoichiometry.

The degree of disorder can be expressed by the Boltzmann equation, which was designed to evaluate lattice entropy. In the case of a large degree of disorder, we can anticipate that lattice entropy increases when the DPT degree increases.

$$S = k \ln W = k \ln(W_{A1} \times W_{A2}) = k(\ln W_{A1} + \ln W_{A2}), \quad (3)$$

Where S is the entropy of the system, k is the Boltzmann constant, and W, W_{A1} and W_{A2} are the number of ways of distribution of the total A site, A1 site, and A2 site, respectively. The numbers W_{A1} and W_{A2} can be calculated theoretically by using the number of Ba and Na ions and vacancies in the A1 and A2 sites. Consequently, the entropy can be calculated by the Ba–Na ratio [16].

The number of ways of distribution of the total A sites with respect to the Ba–Na ratio is also expressed in Fig. 7. The number of ways of distribution was calculated for 1,000 unit cells. In this system, the number of distributions marked the minimum value at the stoichiometry of $x = 1.0$. This tendency shows a similarity with the DPT behavior as depicted in Fig. 7.

Conclusion

In tungsten bronze structured $Ba_2NaNb_5O_{15}$ ceramics, densification of the Ba excess samples was higher than that of the Na excess samples due to the cation vacancies in Ba excess samples, which provided easier diffusion paths. On the other hand, the maximum dielectric constant and the Curie temperature show the highest values at the stoichiometric composition and those values decreased as the composition went away from the stoichiometry. For a quantitative evaluation of DPT behavior of the BNN ceramics, γ and C/κ_{max} were calculated. The weakest DPT behavior was observed in the stoichiometric composition. An increased DPT is in correlation with the increase in the number of ways of distributions by the disordered occupation of Ba, Na and vacancies in the A1 and A2 sites.

Acknowledgements This work was supported by grants No. R01-2003-000-11606-0 from the Basic Research Program of the Korea Science and Engineering Foundation.

References

1. Xu Y (1991) Ferroelectric materials and their applications. Elsevier, North-Holland
2. Francombe MH (1960) Acta Cryst 13:131
3. Liu JM, Zhu SN, Liu ZG, Zhu YY, Wu ZC, Ming NB (1995) Solid State Commun 93:479
4. Giess EA, Scott BA, Burns G, O'kane DF, Segmuller A (1969) J Am Ceram Soc 52:276
5. Singh S, Draegert DA, Geusic JE (1970) Phys Rev B 2:2709
6. Yoshikawa A, Itagaki H, Fukuda T, Lebbou K, El Hassouni A, Brenier A, Goutaudier C, Tillement O, Boulon G (2003) J Cryst Growth 247:148
7. Rao KS, Yoon KH (2003) J Mater Sci 38:391
8. Fullmann RL (1953) Trans AIME 3:447
9. Scott BA, Giess EA, O'Kane DF (1969) J Mater Sci 4:107
10. Carruthers JR, Grasso M. (1969) Mater Res Bull 4:413
11. Shafer MW, Roy R(1959) J Am Ceram Soc 42:485
12. Uchino K, Nomura S (1982) Ferroelectric Lett Sect 44:55
13. Butcher SJ, Thomas NW (1991) J Phys Chem Solids 52:595
14. Cross LE (1987) Ferroelectrics 76:241
15. Cross LE (1994) Ferroelectrics 151:305
16. Kim MS, Wang P, Lee JH, Kim JJ, Lee HY, Cho SH (2002) Jpn J Appl Phys 41:7042